IL NUOVO CIMENTO Vol. 30 C, N. 5 Settembre-Ottobre 2007
DOI 10.1393/ncc/i2008-10265-9

First results on SiPM characterization within the FACTOR experiment(*)

V. Bonvicini(**), L. Bosisio, D. Cauz, A. Driutti, G. Pauletta, A. Penzo, I. Rashevskaya, A. Vacchi and E. Vallazza

INFN, Sezione di Trieste - Via A. Valerio 2, 34127 Trieste, Italy

(ricevuto il 3 Marzo 2008; pubblicato online il 29 Aprile 2008)

Summary. — Silicon Photo-Multipliers (SiPMs) are nowadays considered, thanks to their peculiar characteristics, very promising devices for many different applications requiring fast, reliable and compact photodetectors with single-photon counting capability. In the framework of the INFN R&D project FACTOR (Fiber Apparatus for Calorimetry and Tracking with Optoelectronic Read-out), we present in this paper results on different measurements performed on several SiPMs, produced by FBK-irst (Trento, Italy) and by Obninsk/CPTA (Moscow, Russia). Fundamental SiPMs parameters, such as breakdown voltage (V_{BD}), gain and dark count rate are compared for the different devices. Results about the study of the dependence of both V_{BD} and dark count rate on temperature (in the range 0–50 °C) are also given. Finally, results from a preliminary beam test of a 1 m long scintillator bar read out by a wls fibre coupled to two FBK-irst SiPMs are presented.

PACS 85.30.-z – Semiconductor devices.
PACS 85.60.Dw – Photodiodes; phototransistors; photoresistors.
PACS 29.40.Vj – Calorimeters.

1. – Introduction and motivation

Silicon Photo-Multipliers (SiPMs) have been receiving a growing attention in the last years as they are considered an extremely promising replacement for traditional photomultiplier tubes (PMTs) for the detection of low-intensity light levels in many fields of application (see, *e.g.*, [1] and references therein). The device is based on a matrix of small, passive-quenched silicon avalanche photodiodes operated in limited Geiger-mode (GM-APDs) and read out in parallel from a common output node. Each element (referred to as either "microcell", "μcell" or "pixel") gives the same current response when

(*) Paper presented at the 1st Workshop on Photon Detection for High Energy Medical and Space Applications; Perugia, June 13-14, 2007.
(**) E-mail: bonvicini@ts.infn.it

hit by a photon, hence the total output signal is proportional (for moderate fluxes) to the number of hit μcells. The advantages of SiPMs over conventional PMTs are numerous: insensitivity to magnetic fields, low-voltage operation, low power consumption, comptactness and low cost.

FACTOR (Fiber Apparatus for Calorimetry and Tracking with Optoelectronic Readout) is an INFN 3-year R&D project started at the beginning of 2007. The birth of this project was motivated by a strong interest for both the development of the device itself and for its future applications, especially to the readout of fibre calorimeters in High Energy Physics (HEP) and to the detection of photons emitted by Ultra High Energy Cosmic Rays (UHECR) during atmospheric showers. FACTOR's experimental program foresees an active collaboration with ITC-irst (recently Fondazione Bruno Kessler, FBK-irst, Trento, Italy). The first year of the project (2007) is being mainly dedicated to device characterization and analysis. In particular, the first objective of FACTOR is the achievement of a thorough understanding of both capabilities and limits of SiPMs by studying, measuring and comparing, in different environmental conditions, the most critical device parameters for SiPMs fabricated by different producers.

In this paper we present the first experimental results obtained by the FACTOR Collaboration in the first months of activity. Section **2** summarizes the characteristics of the SiPMs analyzed up to now and describes the experimental set-up used for the measurements. Section **3** illustrates the experimental results obtained so far. In particular, static (forward and reverse I-V) and dynamic (in dark) measurements have been performed. Signal shape and amplitude, dark count rate and gain have been analyzed. The dependence of the SiPM breakdown voltage (V_{BD}) and of the dark count rate on temperature have also been investigated. Section **4** reports on the results of a preliminary application study performed by reading out with two SiPMs fabricated by FBK-irst a wls fiber coupled to a 1 m long polystyrene scintillator bar on a test beam with high-energy protons at Fermilab. Finally, an outlook to the future experimental activity of FACTOR is given in sect. **5**.

2. – Experimental

2·1. *Devices under test.* – The results presented in this paper were obtained with devices procured from 3 different sources: FBK-irst [2], Photonique [3] and Forimtech [4]. The latter two are distributors for CPTA-Obninsk, one of the original developers of SiPMs [5], while FBK-irst design and process their own devices. The DUTs (Devices Under Test) have different characteristics and dimensions, which are summarized in table I.

It can be noticed from table I that FBK-irst devices have polysilicon-made quenching resistors (R_{q}), while the Russian SiPMs are characterized by quenching resistors realized with the Metal-Resistive-Semiconductor (MRS) technology developed at CPTA [5].

2·2. *Measurement set-up.* – Both static and dynamic characterizations have been carried out in dark condition and on packaged devices. Forimtech and Photonique SiPMs come already packaged in different cases (see table I), while the devices we received from FBK-irst were naked dies which had been previously diced from the wafers. We therefore glued each of them on top of empty TO18 cases (using a conductive epoxy) and wire-bonded the output pad to a case pin (see fig. 1).

The functional (dynamic) characterization at room temperature of the devices has been carried on with a simple set-up: the DUT was mounted onto a prototype printed

TABLE I. – *Summary of the principal characteristics of the measured SiPMs.*

Producer:	Forimtech (CPTA)	Photonique (CPTA)	Photonique (CPTA)	Photonique (CPTA)	FBK-IRST
Quenching resistor:	MRS	MRS	MRS	MRS	Polysilicon
Device area:	$1\,mm^2$	$1\,mm^2$	$1\,mm^2$	$4.4\,mm^2$	$1\,mm^2$
No. of μcells:	556	556	556	1748	625
μcell area:	$43\times43\,\mu m^2$	$43\times43\,\mu m^2$	$43\times43\,\mu m^2$	$50\times50\,\mu m^2$	$40\times40\,\mu m^2$
Peak wavelength:	560 nm	600 nm	440 nm	440 nm	420 nm
Packaging:	TO18	TO18	TO18	PCB	TO18
# of devices tested:	5	4	2	3	12
Notes:	Green-Red sensitive	Green-Red sensitive. Model 050701GR_TO18	Blue sensitive Model 0611B1MM_TO18	Blue sensitive Model 0611B4MM_TO18	Devices belonging to several wafers with different processes

circuit board together with a commercial broad-band RFIC amplifier (ABA-52563 by Avago Technologies [6]). This amplifier provides a gain of about 20 dB with a flat broad-band response from 10 MHz to 3.5 GHz. These characteristics are well suited for studying the extremely fast signals of SiPMs, whose rise time is of the order of a few hundreds of ps. The amplifier is internally 50-ohm matched and is available in a small sized ($\sim 1.8\times1.8\,mm^2$), 6 lead SOT-363 surface mount plastic package.

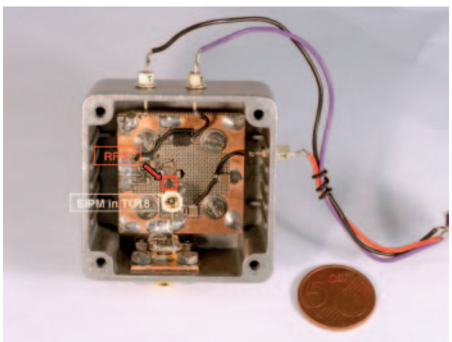

Fig. 1. – Picture showing the prototype printed circuit board housing a $1\,mm^2$ SiPM (mounted on a TO18 case) and the RFIC amplifier.

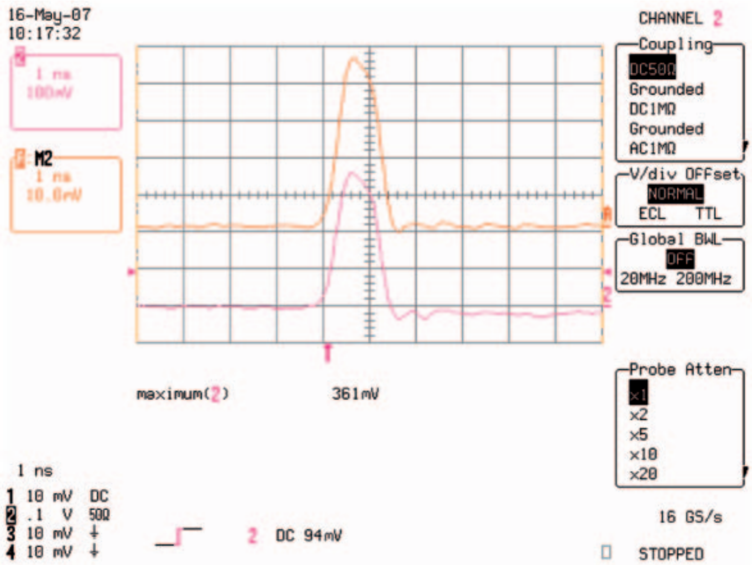

Fig. 2. – (Colour on-line) Characterization of the RFIC amplifier performance: DSO picture showing the amplifier's response (red trace) to an input signal (orange trace) from a pulse generator.

Before starting the SiPM dynamic measurements, the amplifier was carefully characterized and tested. The gain *vs.* frequency characteristics was measured with a spectrum analyzer, for a frequency sweep of the input signal from 10 MHz to 1.8 GHz (upper frequency limit of the spectrum analyzer) and the flatness of the amplifier's response in this frequency range was found consistent with the manufacturer's specifications. The measured voltage gain in this frequency range is about 18 dB, *i.e.* ~ 8. The dynamic behaviour of the amplifier was tested with a pulse generator. As an example, fig. 2 shows the response (red trace) of the amplifier to an input signal pulse (orange trace) having 0.9 ns FWHM, rise time = fall time (10–90%) = 300 ps and an amplitude of 45 mV.

3. – Results

3·1. *Static characterization.* – Static measurements carry a great deal of information, as they permit, on the one hand, to quickly select good from bad devices, and, on the other hand, to extract almost immediately important device parameters, such as the breakdown voltage ($V_{\rm BD}$), the average value of the quenching resistors and, for a device with a known gain, the dark count rate (or vice versa).

As for a normal *p-n* diode, a SiPM (which, as already stated in sect. **1**, is a matrix of independent GM-APDs connected in parallel) can be biased in forward and in reverse polarity. Figure 3 shows a set of forward *I-V* measurements performed on 6 FBK-irst devices (see table I for the device characteristics). The forward *I-V* characteristics can be divided into two regions [7]. A first region (up to a few hundreds mV of forward bias), in which the current is essentially determined by the parallel of the diode equivalent resistances of the individual μcells and, therefore, the current exhibits an exponential dependence on V. A second region (beyond ~ 0.5 V), in which the current exhibits a

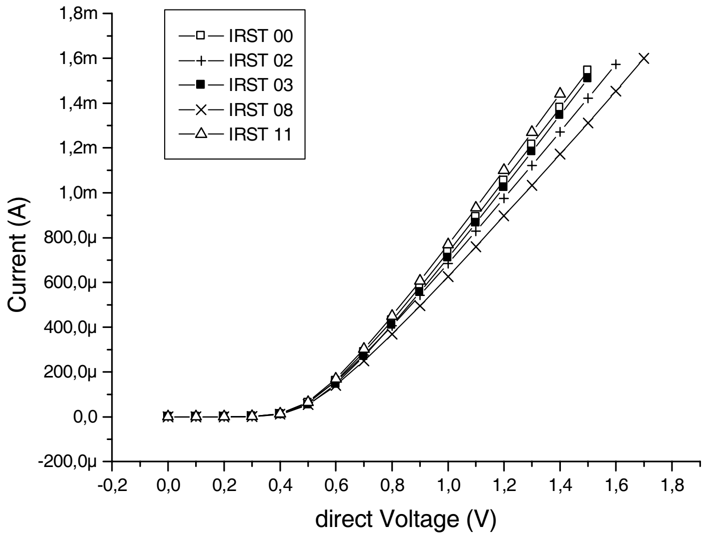

Fig. 3. – Forward I-V curves for a set of 5 FBK-irst devices.

linear dependence on the bias voltage V. The reason for this behaviour is that in this second region the current becomes governed by the quenching resistors of the μcells, which now dominate over the diode equivalent resistances. Therefore, a linear fit of this second region allows to extract the value of the parallel of the quenching resistors of the individual μcells. Knowing the number of μcells in the structure, one can calculate the average value of the single quenching resistor R_q. For FBK-irst devices (polysilicon resistors) values of R_q ranging from ~ 400 to $\sim 650\,\mathrm{k}\Omega$ were found, pretty uniform among devices of the same batch.

Much higher R_q values were measured for both Forimtech and Photonique SiPMs, whose quenching resistors are fabricated with the Metal-Resistive-Semicondictor technology. In general, we have observed that MRS SiPMs displayed values of R_q from about 2 to 50 times larger than FBK-irst devices. Such large values of quenching resistance, if, on the one hand, ensure a very effective avalanche quenching, on the other hand imply a longer recovery time for the SiPM signals, whose exponential decay is governed by the time constant $\tau = R_\mathrm{q}C_\mathrm{D}$ (where C_D is the μcell diode capacitance) and therefore limit the rate at which the device can be operated. Conversely, an advantage of MRS devices over polysilicon resistor SiPMs is that the area occupied by the resistor is smaller for the former technology, so that the fill factor is higher.

Reverse I-V measurements were performed on all devices listed in table I. This measurement allows to extract, first of all, the V_BD of the devices. As an example, fig. 4 shows the results of a reverse I-V measurement performed on 5 FBK-irst devices. It is clear from the plot that V_BD is around 33 V. Again, we found pretty uniform V_BD values for SiPMs belonging to the same batch.

Moreover, the DC current value above breakdown provides information on the dark count rate and/or the device gain. In fact, since the current is the average charge flowing through the junction in 1 s, in an ideal device it is given by the charge contained in one pulse (Q) multiplied by the number of pulses per second (dark count) [7]. The first term is the gain of the device, that is the number of carriers created by the single charge carrier

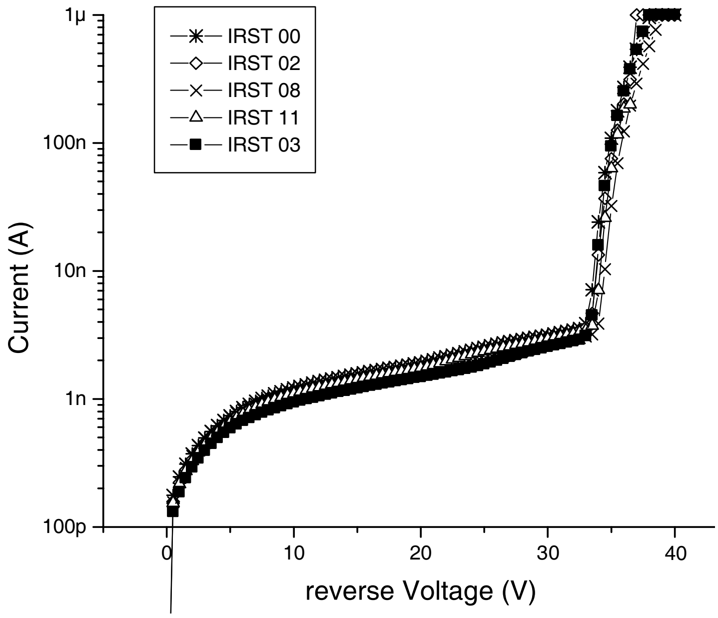

Fig. 4. – Reverse I-V curves for the same SiPMs of fig. 3.

that triggered the avalanche. Therefore, by measuring, for instance, the dark count rate (see next subsection), it is possible from the value of the DC current above breakdown to extract the gain of the device for that value of overvoltage.

3˙2. *Dynamic characterization in dark at room temperature.* – The dynamic characterization of the devices has been done in dark conditions, using the amplifier described in subsect. **2**˙2. In dark, the SiPM signals are obviously due to thermally generated carriers that trigger an avalanche when traversing the high-field region of the device. Figure 5 shows two closely occurring dark pulses from a Forimtech device biased at about 4 V above V_{BD} (*i.e.* with an overvoltage $\Delta V = 4\,\mathrm{V}$). The shape of the signal pulse presents, as expected, a very fast rise time ($\sim 280\,\mathrm{ps}$ in this case), which is determined both by the avalanche spreading and by the discharge of the diode capacitance C_{D} through the diode series resistance [7].

Notice that the signal presents a fall time that is much faster ($\sim 2.2\,\mathrm{ns}$ from 90% to 10%) than the slow exponential recovery time expected from the time constant $\tau = R_{\mathrm{q}}C_{\mathrm{D}} \approx 400\,\mathrm{ns}$ for this device. This is due to the bandwith characteristics of the amplifier used, namely its lower $-3\,\mathrm{dB}$ frequency of about 10 MHz that "cuts" the low-frequency components of the signal.

The dark count rate has been measured for all devices as a function of the bias voltage by counting the number of pulses per second. Obviously, dark count is one of the most critical issues for some SiPM applications, especially for large area devices, as it poses limits to the detection of very small light intensities (one or a few photoelectrons). Figure 6 shows the measured dark count rate for the 5 Forimtech devices (Green-Red sensitive, area $1\,\mathrm{mm}^2$). These devices, which have $V_{\mathrm{BD}} \approx 20\,\mathrm{V}$, present uniform values of dark count rate, featuring values around 2 MHz at $\Delta V = 2\,\mathrm{V}$.

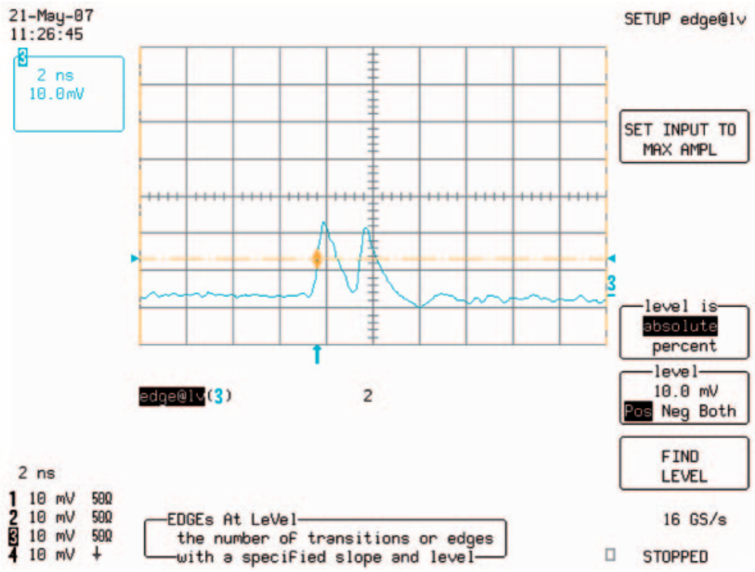

Fig. 5. – DSO image of two dark pulses from a Forimtech (CPTA) SiPM operated at an over-voltage of 4 V. The rise time of the signals is about 280 ps and their time separation ~ 2 ns.

A very similar behaviour has been found also for the Photonique green-red–sensitive devices of the same area.

On the other hand, dark count measurement performed on blue-sensitive devices from Photonique have shown that the dark count rate in these devices increases dramatically after breakdown.

This is clearly shown in fig. 7, which shows the dark count measured on 2 Photonique

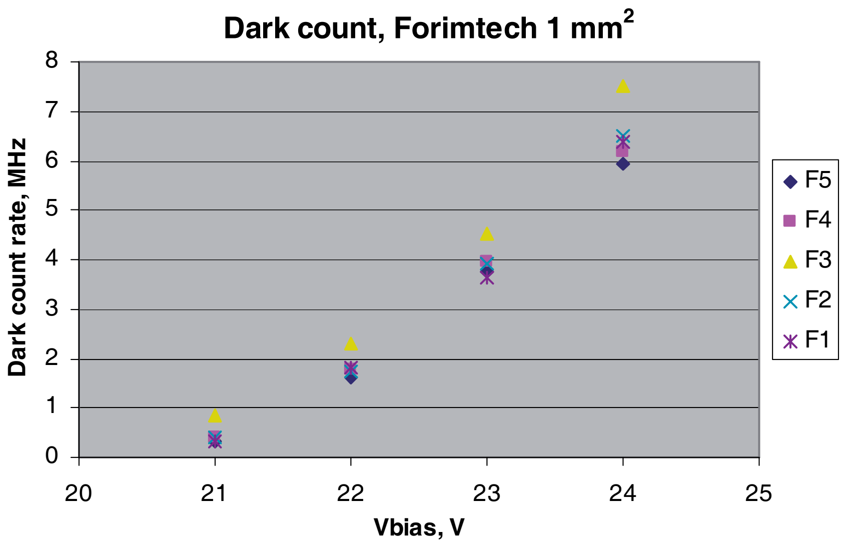

Fig. 6. – Dark count rate (at room temperature) measured on 5 Forimtech (CPTA) devices.

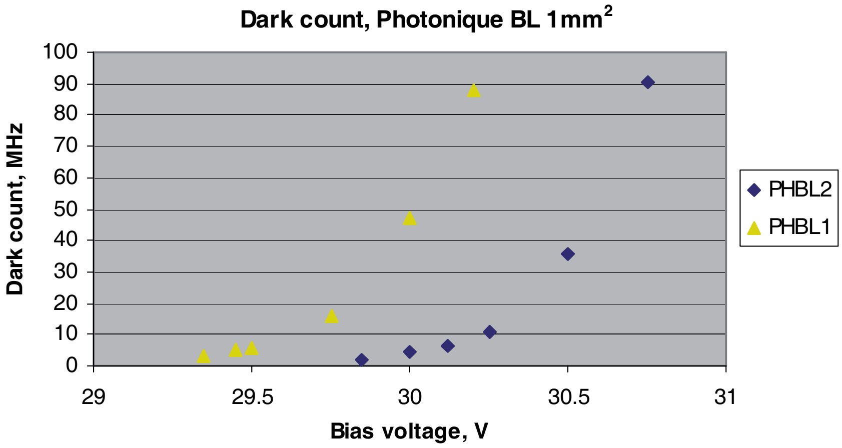

Fig. 7. – Dark count rate (at room temperature) measured on 2 Photonique (CPTA) "Blue sensitive" devices (mod. SSPM_0611B1MM_TO18).

blue-sensitive device with area 1 mm^2. It is clear from these curves that in order to keep the dark count rate at acceptable levels (say, a few MHz), the devices must be operated barely above V_{BD}, which means that the SiPM gain will consequently be quite low.

Figure 8 reports the measured dark count on 5 FBK-irst SiPMs belonging to different batches. Since V_{BD} was not the same for the different devices, the results have been "normalized" to the effective overvoltage at which each device was operated, so that all results could be displayed on the same plot.

In general, the dark rates for FBK-irst devices were, on average, lower (for a given overvoltage) than those of the other SiPMs.

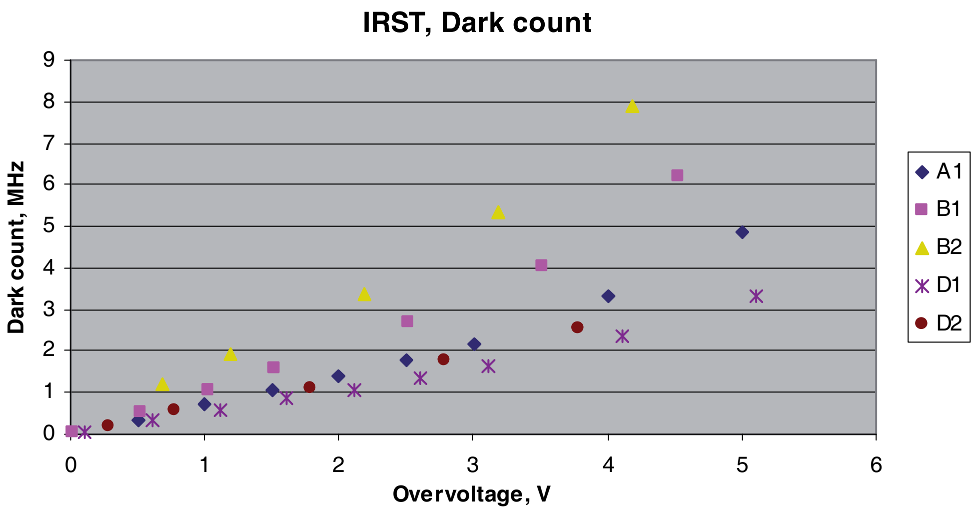

Fig. 8. – Dark count rates (at room temperature) measured on 5 FBK-irst devices belonging to different fabrication batches.

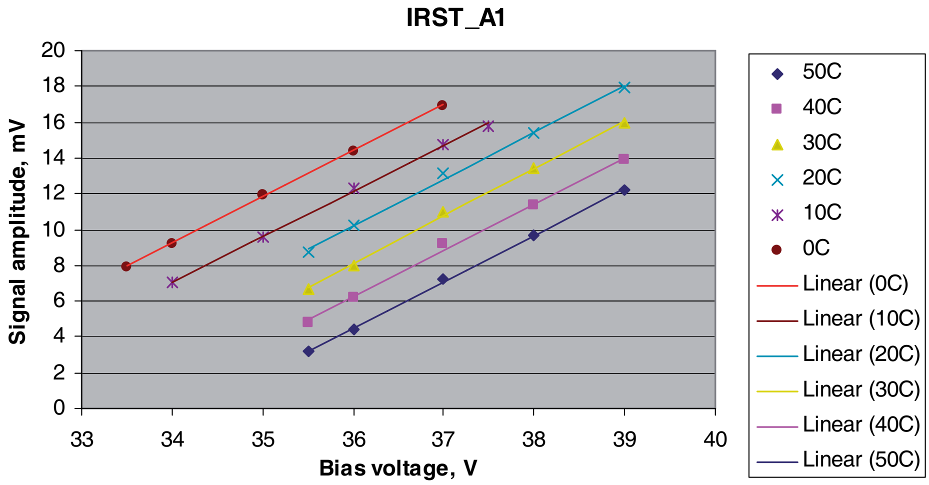

Fig. 9. – Signal amplitude as a function of the bias voltage measured for an FBK-irst SiPM at 6 different temperatures (from 0 °C to 50 °C).

3˙3. *Temperature effects*. – The evaluation of the effects of temperature variations on the characteristics and performance of SiPMs is an important item in view of their experimental applications. Some applications (*e.g.*, space experiments) may require the devices to operate over a wide range of temperatures. On the other hand, other applications that require low levels of dark count might benefit from its reduction through low-temperature operation of the device. Finally, also V_{BD} and gain are inherently dependent on T and therefore it is important to study, understand and (possibly) parametrize their dependence.

The measurements were performed by placing the shielded box containing the DUT in a climatic cabinet with humidity control. To avoid coupling the effects of temperature variations on the amplifier with the effects on the SiPM itself, the amplifier was located outside the climatic chamber. The DUT was connected to the amplifier via a special, 50 Ω microwave cable (operating frequency 18 GHz, temperature range −55 °C to +105 °C). A thermocouple placed inside the DUT box allowed to measure the effective air temperature inside the box in the vicinity of the SiPM.

Figure 9 shows the results obtained on an FBK-irst device measuring the signal amplitude as a function of the applied bias voltage, for 6 temperatures (0 °C, 10 °C, 20 °C, 30 °C, 40 °C and 50 °C). We see that the signal amplitude decreases, for a given bias voltage, when the temperature is increased.

This is due to the fact that the breakdown voltage V_{BD} increases with temperature and therefore the effective overvoltage ($\Delta V = V_{\mathrm{BIAS}} - V_{\mathrm{BD}}$) decreases. This effect is indeed what is expected in case of junction breakdown dominated by the avalanche effect, because when T increases the mean free path of the charge carriers decreases, hence the mean energy acquired from the applied field by a carrier between two consecutive collisions decreases also (see, *e.g.*, [8]).

In fig. 9, the breakdown voltage of the SiPM for each temperature value can be found from the intercept of the linear fit of each set of points with the voltage axis. By plotting the V_{BD} values thus obtained as a function of T, the plot of fig. 10 is obtained.

A linear fit gives a coefficient of specific variation with T of about 78 mV/°C. Very similar results were found for all FBK-irst devices. Measurements performed on Forimtech

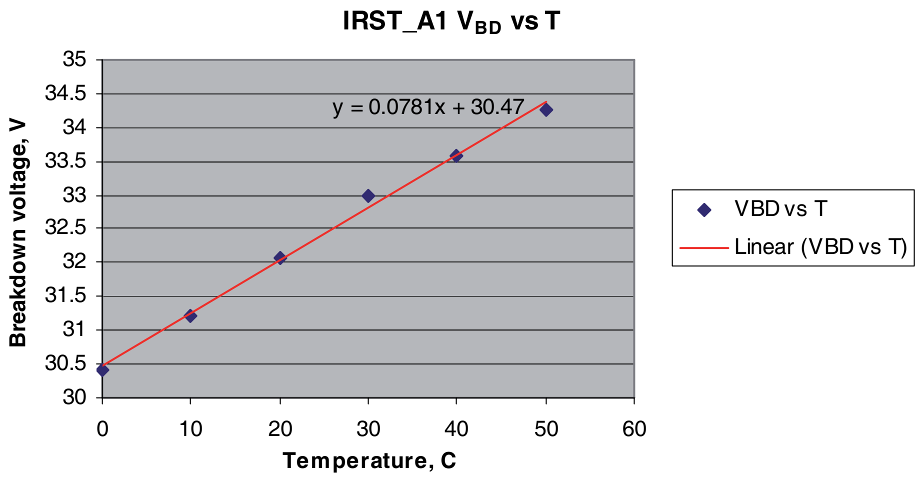

Fig. 10. – Variation of V_{BD} with temperature for the same device of fig. 9.

SiPMs, on the other hand, gave a significantly different dependence of V_{BD} *vs.* T. Figures 11 and 12 are the equivalent of figs. 9 and 10, respectively, for a Forimtech device.

From fig. 12 we see that the temperature coefficient of V_{BD} for the Forimtech device is $\sim 13\,\text{mV}/^{\circ}\text{C}$, *i.e.* about 6 times less than that found for the FBK-irst device. Further investigation and measurements are needed to explain such a large difference. One possible explanation could be that in the Forimtech devices there is a small (though non-negligible) contribution of the Zener effect (direct transition of electrons from the valence band to the conduction band via tunneling through the potential barrier) to the breakdown mechanism. To verify this hypothesis, the measurements should be extended toward lower temperature values. This work is currently under way.

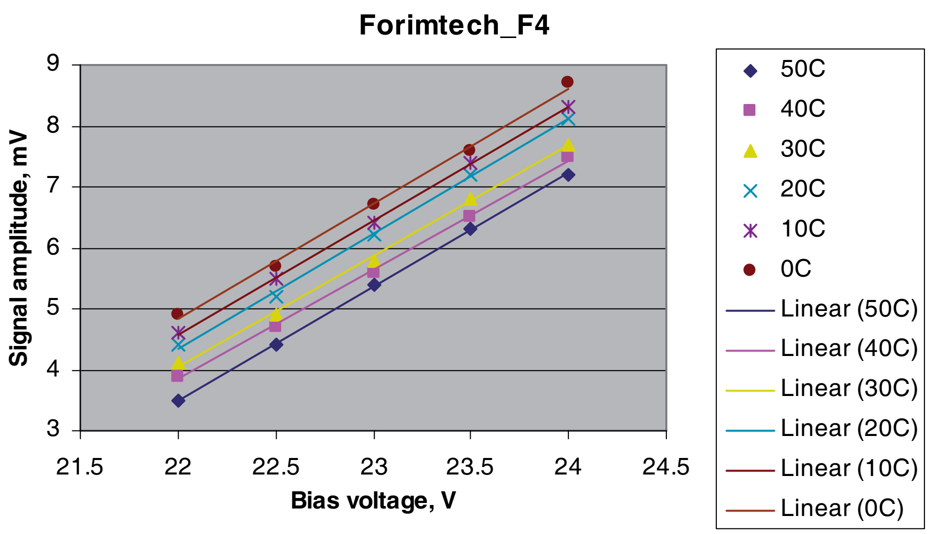

Fig. 11. – Signal amplitude as a function of the bias voltage measured for a Forimtech (CPTA) SiPM at 6 different temperatures (from 0 °C to 50 °C).

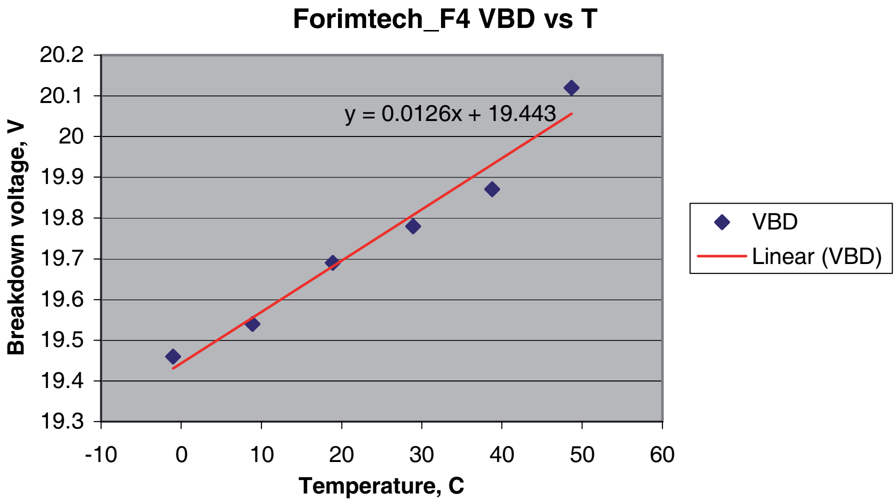

Fig. 12. – Variation of V_{BD} with temperature for the same device of fig. 11.

The dark count rate, being primarily due to thermally generated charge carriers that trigger an avalanche when passing through the high-field region, is obviously expected to decrease significantly with temperature. Figure 13 is a plot of the measured dark count rate, at different temperatures, as a function of the effective overvoltage ΔV at which the device was being operated.

The results show that at $0\,^{\circ}\mathrm{C}$ the dark count rate is about 200 kHz at $\Delta V = 2\,\mathrm{V}$ and about 0.75 MHz at $\Delta V = 5.5\,\mathrm{V}$.

Figure 14 shows a similar plot obtained, for the same set of temperatures, for a Forimtech device. The results presented for these two devices are typical of the general behaviour of all measured FBK-irst and green-red–sensitive MRS-type SiPMs.

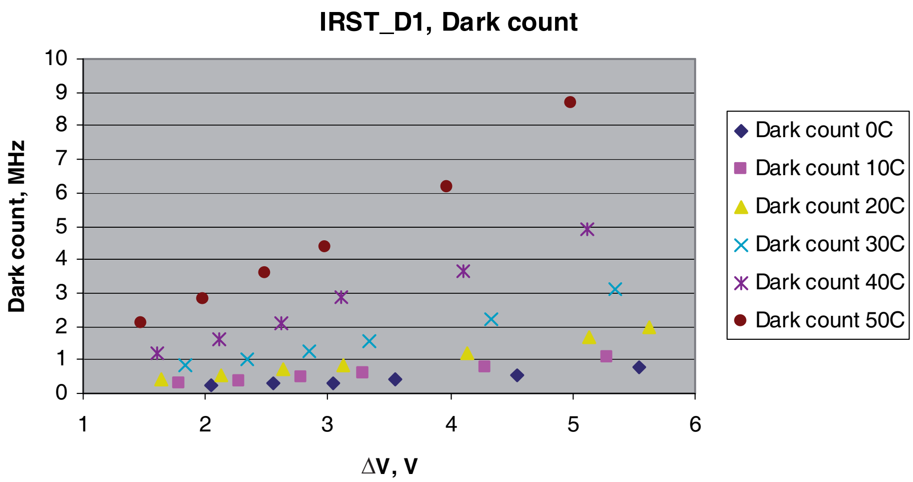

Fig. 13. – Dark count rate at different temperatures for an FBK-irst device.

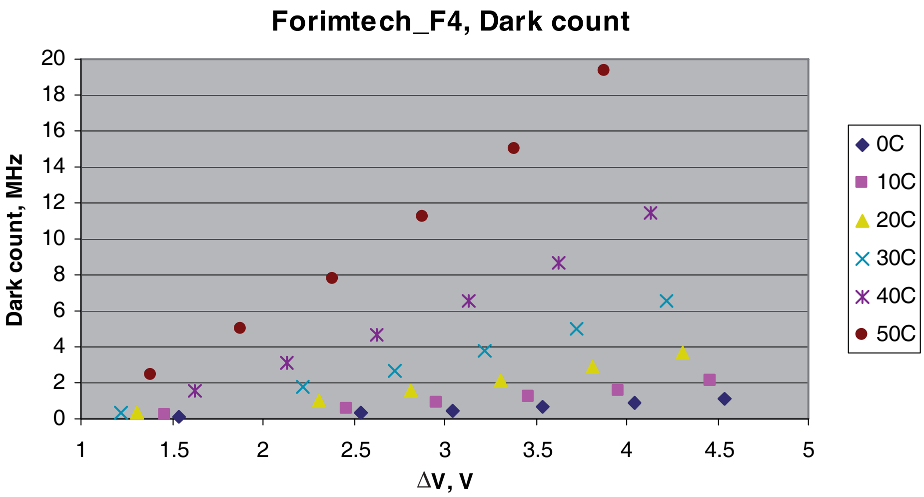

Fig. 14. – Dark count rate at different temperatures for a Forimtech (CPTA) device.

4. – A preliminary application study

In view of the interest for the application of SiPMs to the readout of scintillators in calorimetry, a preliminary test was conducted at FNAL by placing on a high-energy (60 GeV/c and 120 GeV/c) proton beam a 1 m long polystyrene scintillator bar. The bar used a 1 mm diameter wavelength-shifting (wls) fibre cemented in a 2 mm diameter

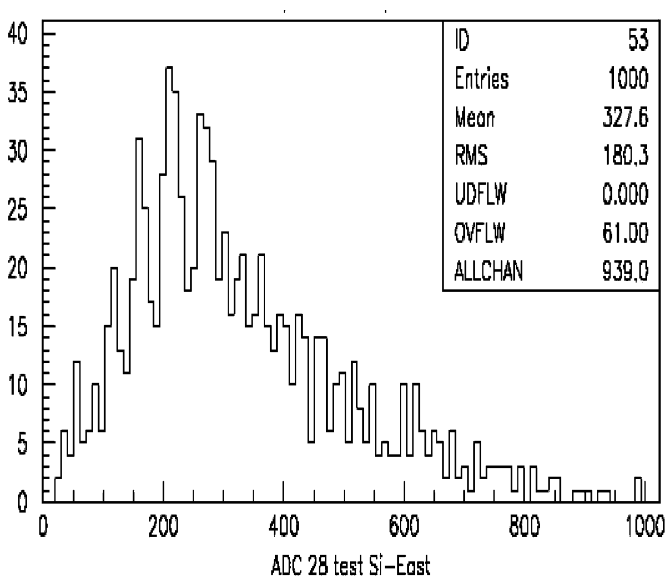

Fig. 15. – Plot of the signal distribution from one of the two FBK-irst SiPMs used to read out the scintillator bar with wls fibre during the beam test at FNAL (data from a proton run at 120 GeV/c).

groove at the centre of the bar to collect and transport the light. The wls fibre was read out, at both ends, by 2 SiPM by FBK-irst. The scintillator bar was placed in front of a large muon counter array made up of similar scintillator bars read out by multi-anode PMTs. The test gave very encouraging results. In fact, the performances of the SiPMs in operating conditions were equal to those measured in the preliminary tests in the laboratory (*i.e.* Gain $\approx 1.6 \times 10^6$ and Dark count $\approx 1.5\,\text{MHz}$ at $\Delta V = 2\,\text{V}$). Despite the fact that the alignment of the fibre with the SiPMs (which, having roughly the same dimensions, was critical) was done without the use of proper tools, the test gave a measured efficiency of 99% at $\Delta V = 2\,\text{V}$. In the same conditions, the mean number of photoelectron per MIP (Minimum Ionizing Particle) was ~ 6.5. Figure 15 plots a signal distribution from one of the two SiPMs for one run at 120 GeV/c.

5. – Outlook

The experimental program of the FACTOR project for the remaining part of 2007 will focus on the completion of the measurements of SiPM parameters currently under way, especially concerning the study of the variation of the SiPM gain with temperature. We also plan to extend the test and comparison of SiPMs to devices from other producers (such as Hamamatsu, MEPHI/Pulsar, etc.). Besides the measurements described in the paper, also the timing resolution and the Photo-Detection Efficiency (PDE) of the different devices will be measured.

The measurement set-up will be improved: a new version of the amplifying circuit, employing 2 cascaded RFICs, is already under test. The new circuit will have higher gain and lower $-3\,\text{dB}$ roll-off frequency, thus extending the bandwith toward low frequencies.

Another important item that will be addressed in the next months concerns the study of radiation effects on SiPMs. The knowledge of radiation damage effects on the SiPM parameters is of paramount importance for all experimental applications and, at the moment, very few data are available in the literature on this argument.

Finally, we are equipping a full plane of 64 scintillator bars, of the type described in sect. **4**, read out by FBK-irst SiPMs. This plane will be inserted in the neutron counter array of the T956 experiment at FNAL and tested with high-energy proton, pion and electron beams.

REFERENCES

[1] Buzhan P. *et al.*, *ICFA Instrumentation Bulletin*, **23** (2001) 28.
[2] `http://www.itc.it/irst`.
[3] `http://www.photonique.ch/`.
[4] Forimtech SA, Route de Malagnou 32, 1200 Geneve (Switzerland).
[5] Golovin V. *et al.*, *Nucl. Phys. B (Proc. Suppl.)*, **61** (1998) 347.
[6] `http://www.avagotech.com/`.
[7] Piemonte C. *et al.*, *IEEE Trans. Nucl. Sci.*, **54** (2007) 236.
[8] Muller R. S. and Kamins T. I., in *Device Electronics for Integrated Circuits*, 2nd edition (Wiley, New York) 1986.